Simple Manufacture of Surface-Modified Nanolignocellulose Fiber via Vapor-Phase-Assisted Surface Polymerization

Simple Manufacture of Surface-Modified Nanolignocellulose Fiber via Vapor-Phase-Assisted Surface Polymerization

Kubra Eksiler, Yoshito Andou,* and Yoshihito Shirai

Department of Biological Functions and Engineering, Graduate School of Life Science and Systems Engineering, Kyushu Institute of Technology, 2-4 Hibikino, Wakamatsu-ku, Kitakyushu, Fukuoka 808-0196, Japan

S Supporting Information
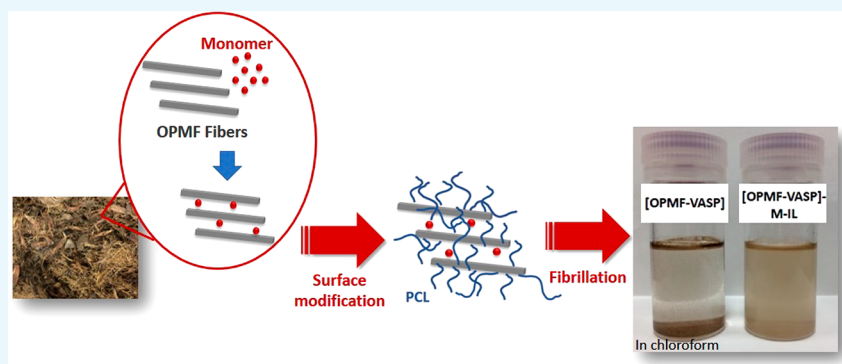
ABSTRACT: This work tackles the disadvantages in the production of functionalized nanofibers from biomass and offers a new methodology to nanofiber-reinforced composite manufacturing. A vapor-phase-assisted surface polymerization (VASP) method has been used to develop surface-modified lignocellulosic nanofibers. Through the vaporized monomers during polymerization, the polymer chains can be introduced deep within oil palm mesocarp fibers (OPMFs) due to their unique porous structure. After OPMFs are modified with polymer chains, the simple Mortar grinder mill−ionic liquid (M-IL) method provides fibrillation from the macro- to nanoscale, retaining the grafted polymer chains. This approach for the functionalization of biomass could lead to the large-scale fabrication of surface-modified nanofibers for reinforced materials and promote innovative implementations of the renewable biomass resource.

1. INTRODUCTION

In the field of materials, biomass has commercial importance and is regarded as a value-added additive.[1] The interest in nanofibers from biomass has been gradually increasing worldwide due to their large specific surface areas.[2] The nanofibers act as a fortification substance by increasing the strength and stiffness, as well as decreasing the weight of the resulting composites.[3] Until biomass turns into nanofiller for the composite, the basic methodology followed by researchers consists of the production of nanofibers from biomass first and then the surface modification of the fibers to avoid agglomeration in a nonpolar polymer matrix.[4−7] Despite vast efforts in this two-stage process, limitations that restrict widespread applications and large-scale manufacturing still build barriers between the composite industry and nanofibers. Moreover, although one of the main reasons to utilize nanofibers as filler is to manufacture eco-friendly composites, the methods commonly used to produce nanofibers are not eco-friendly and require harmful chemicals and a high amount of solvents and time. On the other hand, functionalization of nanofibers also suffers many problems, such as the need for multiple steps, the use of large volumes of organic solvents

where nanofibers do not disperse homogeneously, and the low yield of modified fiber.[8]

The vapor-phase-assisted surface polymerization (VASP) method has been developed to coat many substrate surfaces with polymers, resulting in the conspicuous achievements of control over hydrophobic/hydrophilic properties and surface grafting.[9−16] The VASP process is an excellent method for preserving the delicate surfaces of materials.[17] The polymerization is a solvent-free method, takes place by gas−solid interface interaction, and provides higher grafting rate when compared with the commonly used liquid processes. These benefits make this method appealing to the surface modification of nanofibers.

In modern society, the utilization of biomass as nanofillers in producing advanced materials needs alternative methods with new concepts that could facilitate the processing steps and minimize the use of chemicals. We propose to fulfill these two requirements by combining the oil palm mesocarp fiber (OPMF), a biomass resource with porous structure,[18] grafted
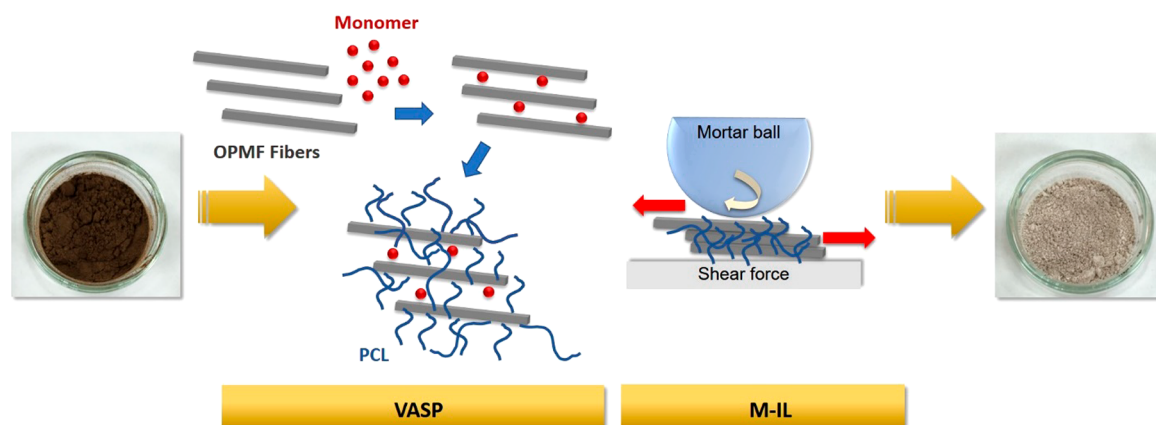
Figure 1. Schematic diagram of the preparation of [OPMF-VASP]-M-IL.

with polycaprolactone (PCL) chains inside the fibers through vaporized monomer molecules, and the Mortar grinder mill-ionic liquid (M-IL) method that was reported as an effective one-step fibrillation procedure in our previous study.[19] Herein, as opposed to the conventional methodology order employed to produce functionalized nanofibers, for the first time in this study, we demonstrate that the fibrillation can be done using functionalized microsize lignocellulose via VASP and yield functional nanoscale materials that have hydrophobic property.

2. RESULTS AND DISCUSSION

VASP of ε-caprolactone was carried out in a H-shaped glass tube reactor on pulverized OPMF. The product, which was named [OPMF-VASP], was similar to a solid layer after the polymerization. On the basis of the increaseed weight of the product over a 24 h period, its composition was estimated to be: fiber 22% and polymer 78%. Afterward, [OPMF-VASP] was treated with a combination method of M-IL to fibrillate the grafted fibers and was called [OPMF-VASP]-M-IL. A schematic illustration of the preparation of functionalized nanofibers is shown in Figure 1.

The changes in the UV/RI intensity ratio of each fraction in size exclusion chromatography (SEC) profiles of the synthesized PCL (M_w 12 000) and the samples, [OPMF-VASP] and [OPMF-VASP]-M-IL, were exhibited in Figure 2. It was found that there is an increment in the UV/RI ratio value of the [OPMF-VASP] sample (Table S1, Supporting Information). In addition, FT-IR results of [OPMF-VASP] and [OPMF-VASP]-M-IL after extraction showed that the peak intensity of the −OH groups associated with the OPMF components margin-ally declined in comparison to that of OPMF (Figure S1, Supporting Information). This result indicates that some OPMF components, such as lignin, were grafted to PCL via covalent bonding. When the combined treatment method of a mortar grinder mill and ionic liquid was employed for the [OPMF-VASP] sample, the treatment led to no change in the PCL-grafted components, revealing the grafted PCL is retained. Moreover, [OPMF-VASP] indicated an increase in the intensity of the PCL carbonyl group peak at 1722 cm^{-1}, whereas the hydroxyl peak of cellulose, hemicellulose, and lignin at 3000−3600 cm^{-1} decreased in comparison to that of OPMF. Another decrease in the peak of C−O−(H) stretching at 1035 cm^{-1} also proved that the grafting of PCL successfully took place on −OH groups of hemicellulose and/or lignin chains. Further-more, it was also found that no significant differences occurred
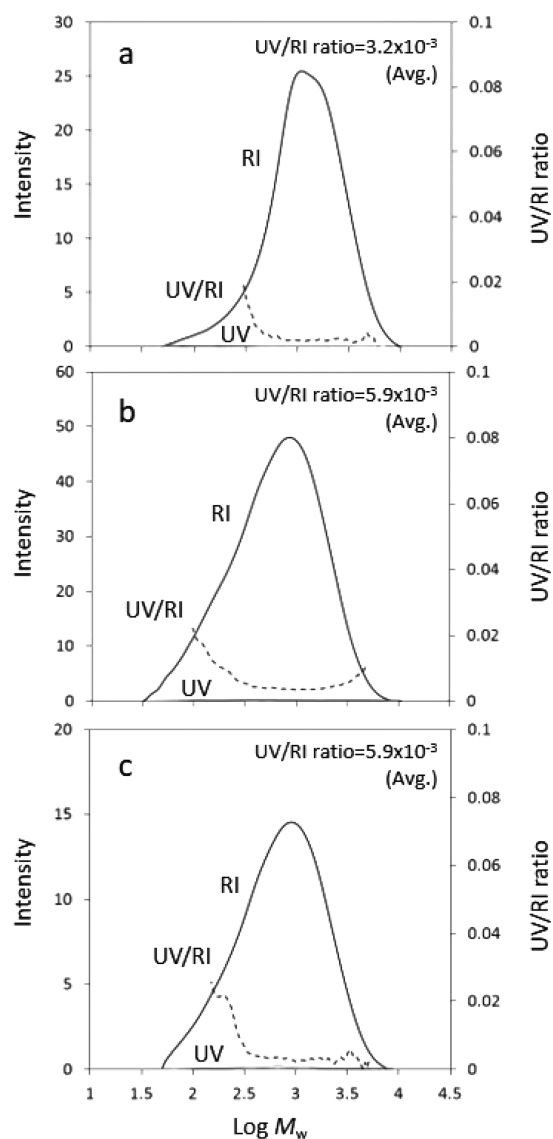

Figure 2. SEC profiles of UV/RI intensity ratios of synthesized PCL (a), [OPMF-VASP] (b), and [OPMF-VASP]-M-IL (c).

between the [OPMF-VASP]-M-IL and [OPMF-VASP] sam-ples after the M-IL treatment, showing that the combined treatment did not destroy the grafted PCL chains of OPMF.

In addition, Figure S2 illustrates the proton nuclear magnetic resonance (^{1}H NMR) spectra of extracted materials of [OPMF-VASP] and [OPMF-VASP]-M-IL when compared to the commercial PCL in order to confirm the formation of the PCL grafting. The same peaks that were found in the commercial PCL were observed in the [OPMF-VASP] sample, apart from 1.24 ppm. This alteration may be attributed to the formation of specific interactions between the fibers and PCL. Furthermore, the characteristic peaks of the commercial PCL were observed in the spectra of [OPMF-VASP]-M-IL, indicating that the M-IL treatment did not cause structural changes on the covalent bonded PCL chains. The additional peaks, perhaps revealing the dissolution of some PCL-grafted components, also remained unaffected. This finding is consistent with the results obtained from FT-IR.

The alteration in the morphology of OPMF was examined by SEM observation. Figure S3a shows the porous structure of OPMF. In Figure S3b, the inset presents the fractured view of the block product, where all the fibers were embedded in PCL after polymerization. On the fractured surface, the marks of interior surface of the fiber were seen, proving that the polymerization occurred for the interior surface of the fiber as well as its external surface. Obviously, after M-IL treatment, the block product of [OPMF-VASP] was pulverized as shown in Figure S3c. The pulverized particles represent that the produced nanofibers were coated and embedded with PCL. In order to confirm the fibrillation, the fractured surface of the PCL composite prepared with 5 wt % [OPMF-VASP]-M-IL loading was observed (Figure S3d, Supporting Information). It was found that the fibers coated with PCL were homogeneously dispersed in the composite matrix. This result is important proof that shows that surface modification of the fibers was done successfully. Size distribution of [OPMF-VASP] before and after the combined treatment was measured through dynamic light scattering (DLS) in Figure 3. The
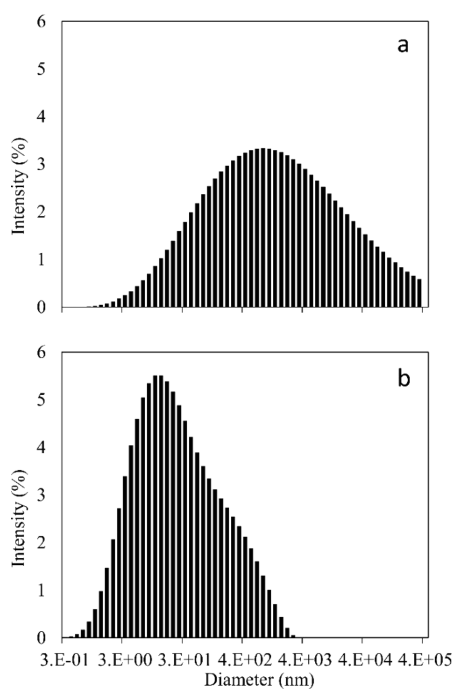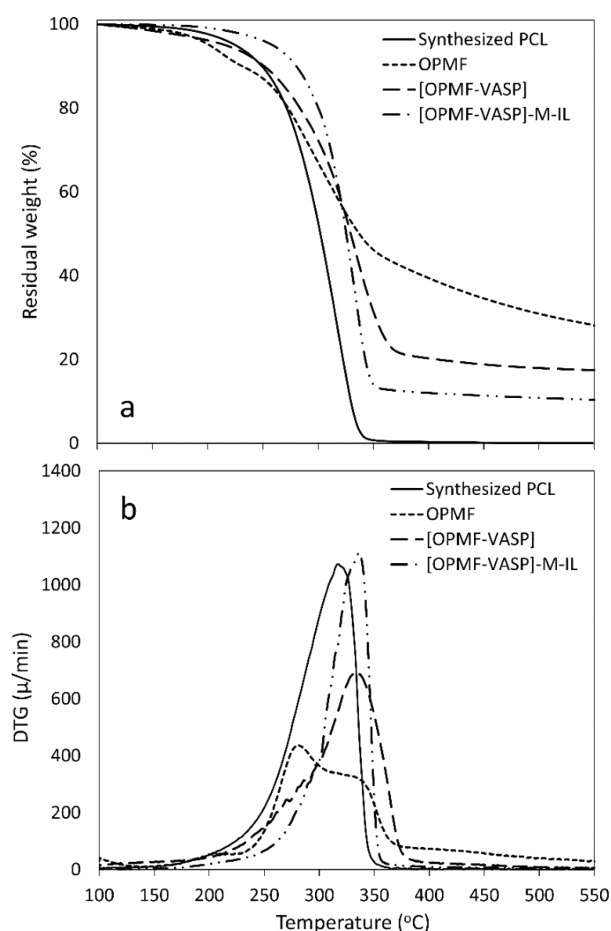
samples were dissolved in toluene and measured at a concentration of 1.03 mg/mL. The measurement of [OPMF-VASP] demonstrated a wide range of size distribution with 16 μm of average diameter. A significant shift to smaller diameters in the size distribution of [OPMF-VASP]-M-IL clearly occurred. This might be due to the fibrillation of the PCL grafted OPMF by mortar grinding, accompanied by the decrease of fiber diameter. In our previous study, we reported that the combination treatment (M-IL) on OPMF also alters the fiber diameter (127 nm), and when ionic liquid dissolves some components of OPMF, the magnetic grinder pulverizes the fiber at the same time.[19] Here, in the case of treatment of [OPMF-VASP], it was reported that the same pulverization effect of the magnetic grinder on the grafted OPMF fibers also provided fibrillation (105 nm). It was expected that the agglomeration of the product particles was inhibited during the wet mortar grinding in the presence of ionic liquid when compared to dry mortar grinding,[20] since the ionic liquid, 1-butyl-3-methylimidazolium fluoroborate ([BMIM][BF4]), facilitates to break down the possible hydrogen bonding among the grafted lignocellulosic components through its poorly coordinated ions. In addition to this, [OPMF-VASP] and [OPMF-VASP]-M-IL were added to chloroform to investigate their dispersion in the organic solvent that PCL can dissolve. The photographs taken before and after 1 h indicate the presence of nanosized fibers after M-IL treatment. It shows a proof of surface modification for nanosized fibers through the VASP method, supporting the DLS results (Figure 4).

Thermogravimetric analysis (TG/DTG) profiles of pulverized OPMF, [OPMF-VASP], and [OPMF-VASP]-M-IL were displayed in Figure 5 to investigate not only the effect of the grafting of PCL on thermal stability of the OPMF but also the effect of M-IL treatment on [OPMF-VASP]-M-IL. It was found that the value of $T_{d50\%}$ of the synthesized PCL was 302 °C, while that of pulverized OPMF was 337 °C. It was clearly observed that the grafted PCL led to a decrease in the thermal stability of [OPMF-VASP] (329 °C). In the DTG curve, the temperature region of 230−320 °C was assigned to the degradation region of a hemicellulose component in the material.[21] Interestingly, the hemicellulose degradation peak of [OPMF-VASP]-M-IL was decreased. This might be explained by the removal of some hemicellulose components during the M-IL treatment. The residual weight difference between [OPMF-VASP] and [OPMF-VASP]-M-IL is also another evidence that reveals the removal of hemicellulose partially from [OPMF-VASP]-M-IL. Therefore, no remarkable difference in the thermal stability of [OPMF-VASP]-M-IL (326 °C) was seen in comparison to [OPMF-VASP]. This result proved that M-IL treatment did not significantly affect the grafted PCL chains on the fibers.

In Figure 6, the Fourier-transform infrared (FT-IR) spectra of ionic liquid residue which was collected after the M-IL treatment of [OPMF-VASP]-M-IL was compared to commercial [BMIM][BF$_4$] ionic liquid. It was observed that it is similar to the spectrum of pure commercial ionic liquid, except for one small extra peak at 1724 cm^{-1} which belongs to the carbonyl group (C=O). This extra peak may be due to the presence of hemicellulose dissolved in ionic liquid. This finding confirms the results obtained from TGA and DTG. Since the FT-IR spectrum confirms that the chemical structure of [BMIM][BF$_4$] remains roughly unchanged during the treatment, it might give an opportunity to reuse the same ionic liquid.

Figure 3. Particle size distribution of the fibers in [OPMF-VASP] (a) and [OPMF-VASP]-M-IL (b).
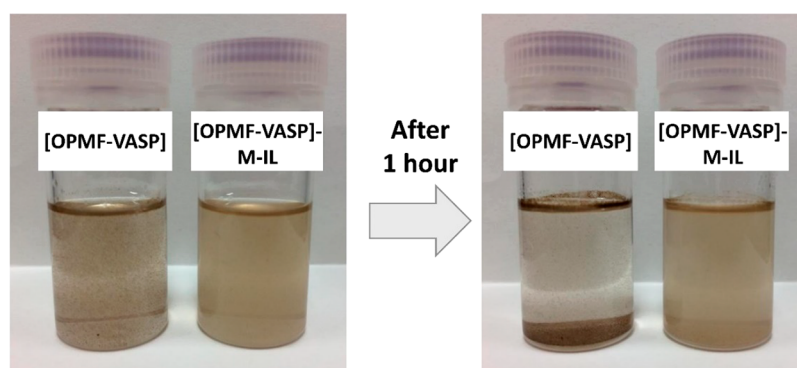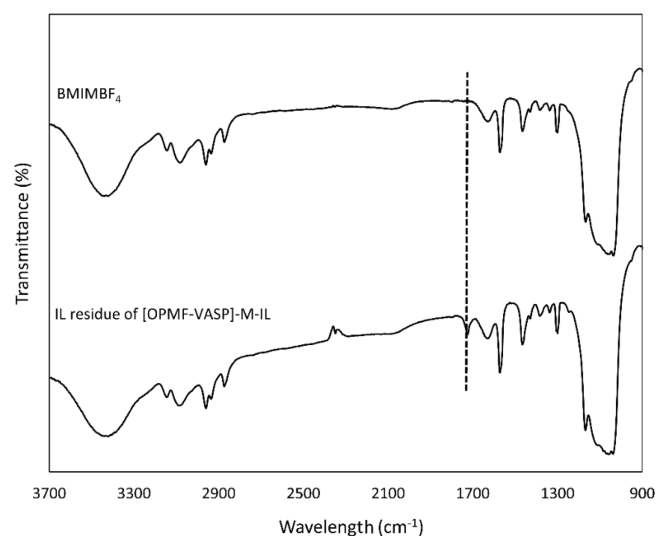
Figure 4. Appearances of [OPMF-VASP] and [OPMF-VASP]-M-IL solutions in chloroform after standing for 1 h.

Figure 5. TG (a) and DTG (b) profiles of the synthesized PCL, OPMF, [OPMF-VASP], and [OPMF-VASP]-M-IL.

Figure 6. FT-IR spectra of the commercial [BMIM][BF$_4$] and the ionic liquid (IL) residue collected after the treatment of [OPMF-VASP]-M-IL.

friendly activities and efforts developed in the field of nanobiomass-based materials. On the other hand, when we perform a chemical modification on biomass and after fibrillation, we bring a new aspect into methodology. A detailed study on the surface-modified nanofiber should be investigated to reveal the potential use of different types of polymers.

4. EXPERIMENTAL SECTION

4.1. Materials. Monomer, ε-caprolactone (>99.0%), was purchased from Tokyo Chemical Industry (Tokyo, Japan). It was dried over calcium hydride (CaH$_2$) (Wako Pure Chemical Industry, Osaka, Japan) and distilled under nitrogen at reduced pressure. Butanol and tin(II) 2-ethylhexanoate (Sn(Oct)$_2$) were obtained from Wako Pure Chemical Industry. Oil palm mesocarp fiber (OPMF) used in this study was obtained from FELDA Serting Hilir Palm Oil Mill, Negeri Sembilan in Malaysia. OPMF was milled using a disc mill (PM-2500M, Osaka Chemical Co., Japan) and sieved (MVS-1N, AS-ONE, Japan) to separate fibers with particle size less than 63 μm, then stored at room temperature in an aluminum bag before use. The ionic liquid, 1-butyl-3-methylimidazolium fluoroborate [BMIM][BF$_4$] (98%), and all the solvents were purchased from Wako Pure Chemical Industry. In order to produce a reference polymer, the bulk polymerization of ε-caprolactone (11.6 mmol) was performed, in the presence of butanol (0.35 mmol,

3. CONCLUSIONS

This paper preliminarily shows the possibility for fibrillation of surface-modified lignocellulose consisting of nanofibers grafted with a hydrophobic polymeric matrix such as PCL. The applicable method to an industrial scale reported in this study avoids the conventional fibrillation methods that require hazardous solvents and eliminates problems which are faced during functionalization of the nanofibers. It should be emphasized that this work builds bridges between two very important research areas related to green chemistry and biomass-based materials. On one hand, the used polymerization approach is closely associated with recent environmentally

initiator) and Sn(Oct)$_2$ (0.06 mmol, catalyst), at 75 °C for 18 h [(M_w = 12 000) calculated by SEC]. Commercial polycaprolactone (PCL) [number-average of molecular weight, M_n = 80 000] was received in pellet form from Sigma-Aldrich.

4.2. Typical Procedure of VASP. Pulverized OPMF (0.2 g) was used as a substrate for VASP, and 0.32 mmol of Sn(Oct)$_2$ was dissolved in 5 mL of acetone. The solution was then mixed with OPMF at room temperature to be absorbed. After it dried under ambient atmosphere, the remaining solvent was removed under vacuum at room temperature. A typical procedure of VASP was done in an H-shaped glass tube reactor with a vacuum cock. The catalyst-supported OPMF was put into a Petri dish, of 4.40 cm^2 bottom surface area, and then the Petri dish was settled at the bottom of one of the legs of the H-shaped glass tube reactor. Purified ε-caprolactone (13.5 mmol) was introduced to the bottom of the other leg. The reactor was then degassed by three freeze−pump−thaw cycles and sealed at last. Polymerization was carried out at 70 °C for 24 h in a thermostatic oven. After VASP, the obtained sample was dried to remove unreactants *in vacuo* and weighted to calculate the weight increment (0.92 g) of the [OPMF-VASP] composite (Table S1).

4.3. Treatment of [OPMF-VASP] Using [BMIM][BF$_4$]. [OPMF-VASP] (1 g) was grinded with 3 mL of [BMIM][BF$_4$] at room temperature for 3 h using a magnetic pestle device (MMPS-T1, AS-ONE, Japan). After the treatment, [OPMF-VASP]-M-IL was washed with ethyl alcohol and centrifuged at 7000 rpm for 20 min (ST 8R, Thermo Scientific, USA).

4.4. Characterization. FT-IR measurements were conducted using a PerkinElmer Spectrum GX Fourier transform infrared (FT-IR) spectrometer. The samples were ground and pelletized using potassium bromide (KBr). The spectra were recorded in the range of 3700−900 cm^{-1} and 16 scans per sample. ^{1}H NMR spectra of the samples were recorded in a 500 MHz JEOL JNM-ECP500 FT-NMR spectrometer in chloroform-*d* at room temperature, and the chemical shifts were reported as δ values (ppm) relative to internal tetramethylsilane (TMS). Thermogravimetric analysis (TGA) was performed using an EXSTAR TG/DTG7000 (SII Nanotechnology Inc., Japan). Approximately 7 mg of sample was placed in an aluminum pan and heated to 550 °C at a rate of 10 °C/min under nitrogen flow (100 mL/min). The particle size distribution was examined by a dynamic light scattering (DLS) (DelsaMax Pro, Beckman Coulter, USA). Measurements were performed at a concentration of 1.03 mg/mL in toluene at 25 °C. Each value was obtained using the average of three measurements. Size-exclusion chromatography (SEC) measurements of the weight-average molecular weight (M_w) and polydispersity index (M_w/M_n) of the polymers obtained after VASP were conducted on a TOSOH HLC-8320 size exclusion chromatograph (Tokyo, Japan) (TSKgel Super HM-H linear column; linearity range, 1×10^3−8×10^6; molecular weight exclusion limit, 4×10^8) using polystyrene as the standard. Polymers were extracted by dissolving in CHCl$_3$ (5 mg/mL). After the dissolution, the solutions were filtered through a membrane filter with 0.45 μm pore size and then measured at a flow of 0.6 mL/min at 40 °C. M_w and M_w/M_n were calculated from the SEC curve using EcoSEC-WS software.

■ ASSOCIATED CONTENT

Ⓢ Supporting Information

The Supporting Information is available free of charge on the ACS Publications website at DOI: 10.1021/acsomega.8b00338.

The ratios of responses of UV and RI detectors of the extracted materials after VASP in SEC analysis and chemical and structural characterization (FT-IR, ^{1}H NMR, and SEM images) (PDF)

■ AUTHOR INFORMATION

Corresponding Author
*E-mail: yando@life.kyutech.ac.jp.
ORCID ⊙
Yoshito Andou: 0000-0003-3839-0705

Notes
The authors declare no competing financial interest.

■ ACKNOWLEDGMENTS

■ REFERENCES

(1) Chartrand, A.; Lavoie, J. M.; Huneault, M. A. Surface modification of microcrystalline cellulose (MCC) and its application in LDPE-based composites. *J. Appl. Polym. Sci.* **2017**, *134*, 44348.

(2) Kang, Y.; Ahn, Y.; Lee, S. H.; Hong, J. H.; Ku, M. K.; Kim, H. Lignocellulosic nanofiber prepared by alkali treatment and electrospinning using ionic liquid. *Fibers Polym.* **2013**, *14*, 530−536.

(3) Menon, M. P.; Selvakumar, R.; Kumar, P. S.; Ramakrishna, S. Extraction and modification of cellulose nanofibers derived from biomass for environmental application. *RSC Adv.* **2017**, *7*, 42750−42773.

(4) Missoum, K.; Belgacem, M. N.; Bras, J. Nanofibrillated Cellulose Surface Modification: A Review. *Materials* **2013**, *6*, 1745−1766.

(5) Habibi, Y. Key advances in the chemical modification of nanocelluloses. *Chem. Soc. Rev.* **2014**, *43*, 1519−1542.

(6) Kalia, S.; Boufi, S.; Celli, A.; Kango, S. Nanofibrillated cellulose: surface modification and potential applications. *Colloid Polym. Sci.* **2014**, *292*, 5−31.

(7) Dufresne, A. Nanocellulose: a new ageless bionanomaterial. *Mater. Today* **2013**, *16*, 220−227.

(8) Hu, Z.; Berry, R. M.; Pelton, R.; Cranston, E. D. One-Pot Water-Based Hydrophobic Surface Modification of Cellulose Nanocrystals Using Plant Polyphenols. *ACS Sustainable Chem. Eng.* **2017**, *5*, 5018−5026.

(9) Kim, D.; Andou, Y.; Shirai, Y.; Nishida, H. Biomass-based composites from poly(lactic acid) and wood flour by vapor-phase assisted surface polymerization. *ACS Appl. Mater. Interfaces* **2011**, *3*, 385−391.

(10) Yasutake, M.; Hiki, S.; Andou, Y.; Nishida, H. Physically Controlled Radical Polymerization of Vaporized Vinyl Monomers on Surfaces. Synthesis of Block Copolymers of Methyl Methacrylate and Styrene with a Conventional Free Radical Initiator. *Macromolecules* **2003**, *36*, 5974−5981.

(11) Nishida, H.; Yamashita, M.; Andou, Y.; Jeong, J. M.; Endo, T. Gas-Phase Assisted Surface Polymerization Behavior of β-Propiolactone on Inorganic and Organic Substrates and Consequent Composite Production. *Macromol. Mater. Eng.* **2005**, *290*, 848−856.

(12) Andou, Y.; Yasutake, M.; Jeong, J. M.; Kaneko, M.; Nishida, H.; Endo, T. Gas-phase-assisted surface polymerization of methyl methacrylate with Fe(0)/TsCl initiator system. *J. Appl. Polym. Sci.* **2007**, *103*, 1879−1886.

(13) Yasutake, M.; Andou, Y.; Hiki, S.; Nishida, H.; Endo, T. Controlled Radical Polymerization of Vaporized Vinyl Monomers on

Solid Surfaces under UV Irradiation. *Macromol. Chem. Phys.* **2004**, *205*, 492−499.

(14) Andou, Y.; Yasutake, M.; Nishida, H.; Endo, T. Designed Surface Modification by Photoinduced Vapor Phase Assisted Surface Polymerization of Vinyl Monomers. *J. Photopolym. Sci. Technol.* **2007**, *20*, 523−528.

(15) Andou, Y.; Yasutake, M.; Jeong, J. M.; Nishida, H.; Endo, T. Gas-Phase Assisted Surface Polymerization of Vinyl Monomers with Fe-Based Initiating Systems. *Macromol. Chem. Phys.* **2006**, *206*, 1778−1783.

(16) Yasutake, M.; Andou, Y.; Hiki, S.; Nishida, H.; Endo, T. Physically controlled, free-radical polymerization of vaporized fluoromonomer on solid surfaces. *J. Polym. Sci., Part A: Polym. Chem.* **2004**, *42*, 2621−2630.

(17) Andou, Y.; Jeong, J. M.; Kaneko, M.; Nishida, H.; Endo, T. Hydrophobic cellulose fiber surfaces modified with 2,2,3,3,3-pentafluoropropylmethacrylate (FMA) by vapor-phase assisted photo polymerization. *Polym. J.* **2010**, *42*, 519−524.

(18) Latif, H. A.; Yahya, M. N.; Zaman, I.; Samb, M.; Ghazali, M. I.; Hatta, M. N. M. Acoustical Characteristics of Oil Palm Mesocarp. *ARPN-JEAS* **2016**, *11*, 7670−7676.

(19) Eksiler, K.; Andou, Y.; Yilmaz, F.; Shirai, Y.; Ariffin, H.; Hassan, M. A. Dynamically controlled fibrillation under combination of ionic liquid with mechanical grinding. *J. Appl. Polym. Sci.* **2017**, *134*, 44469.

(20) Kotake, N.; Kuboki, M.; Kiya, S.; Kanda, Y. Influence of Dry and Wet Grinding Conditions on Fineness and Shape of Particle Size Distribution of Product in a Ball Mill. *Adv. Powder Technol.* **2011**, *22*, 86−92.

(21) Yang, H.; Yan, R.; Chen, H.; Lee, D. H.; Zheng, C. Characteristics of Hemicellulose, Cellulose and Lignin Pyrolysis. *Fuel* **2007**, *86*, 1781−1788.